pH Dependence of actin self-assembly

Fei Wang, Rosemary V. Sampogna, and Bennie R. Ware
Department of Chemistry, Syracuse University, Syracuse, New York 13244

ABSTRACT Fluorescence enhancement and fluorescence photobleaching recovery have been utilized to examine actin self-assembly over the pH range 6.6–8.0. The kinetics of assembly are faster and the critical concentrations are lower at lower pH. Filament diffusion coefficients are not a function of pH, indicating that average filament lengths are not pH dependent. Although critical actin concentrations are a sensitive function of the concentrations of various cations in the medium, the relative pH dependences of critical concentrations are similar for all combinations of cations employed. The pH dependence of actin self-assembly is sufficiently great that it should be taken into account when comparing data from different reports and when relating in vitro measurements to cytoplasmic mechanisms.

INTRODUCTION

Actin self-assembly, originally characterized in research on muscle proteins, is now a subject of vigorous investigation in the field of cytoplasmic motility (Pollard, 1981; Korn, 1982; Oosawa, 1983). When salts are added to the medium, G-actin monomers spontaneously assemble to form F-actin filaments as a result of the association of cations with several sites on the actin molecule (Barany et al., 1962; Martonosi et al., 1964; Strzelecka-Golaszewska et al., 1978). It is presumed that these sites are negatively charged, and thus it may be inferred that a change in pH could alter the assembly process. Although an implicit recognition of the pH dependence of actin self-assembly may be commonplace, there have been no modern investigations in which pH has been an independent variable. The normal control values for pH in recent actin assembly experiments are 7.5, 7.8, and 8.0; and comparisons among different reports generally ignore the differences in the pH of the medium (Selden et al., 1986; Drenckhahn and Pollard, 1986; Carlier et al., 1986; Keiser et al., 1986; Janmey et al., 1986; Zaner and Hartwig, 1988). In the context of cytoplasmic motility, the pH dependence of actin assembly is most interesting over the range of pH encountered in the cytoplasm. Recent advances in the development of optical probes and fluorescence ratio imaging microscopy have permitted accurate determinations of cytoplasmic pH and pH distribution (Nuccitelli and Deamer, 1982; Chaillet et al., 1986; Musgrove et al., 1986, Bright et al., 1987). Excluding the acidic vesicles, the range of pH in cytoplasm is generally bounded by ~6.5–8.0, and there is an emerging interest in the issue of whether the control of pH may be an important component of cytoplasmic regulatory mechanisms (Busa, 1986; Moolenaar, 1986, Frelin et al., 1988).

We report here a characterization of actin self-assembly as a function of pH over the range 6.6–8.0, using several different combinations of cations for induction. Assembly has been characterized by the enhancement of fluorescence of pyrene-labeled actin and by fluorescence photobleaching recovery (FPR) using fluorescein-labeled actin. Both methods were used to measure the kinetics of actin assembly: the former method was used to measure actin critical concentrations, and the latter method was used to measure the diffusion coefficients of actin filaments. For all cation concentrations studied, the results establish a substantial pH dependence of actin self assembly over the cytoplasmic pH range.

Correspondence should be addressed to Dr. Bennie R. Ware.

MATERIALS AND METHODS

Actin was isolated from commercial acetone powder of rabbit muscle (Pel-Freeze Biologicals, Rogers, AR) using a slight modification of the method of Pardee and Spudich (1982), as described previously (Pan and Ware, 1988). The final purification was accomplished by size exclusion chromatography using Sephadex G-150. The central fraction was maintained by dialysis against the appropriate G buffer at 4°C and used for experiments within 3 d of column purification. The concentration of G-actin was determined by absorbance at 290 nm using an extinction coefficient of 0.62 mg^{-1} ml cm^{-1}. Actin was labeled with fluorescein or pyrene using procedures that have been described previously (Pan and Ware, 1988). In both cases the concentration of labeled actin was determined by the method of Hartree (1972) using unlabeled G actin as a standard. For fluorescein label the extent of labeling was determined from the absorbance of the solution of labeled actin at 495 nm, using an extinction coefficient of 6.0×10^4 cm^{-1} M^{-1}. For pyrene the extent of labeling was determined using an extinction coefficient for the label of 2.2×10^4 cm^{-1} M^{-1} at 344 nm. Solutions of labeled and unlabeled actin

0006-3495/89/02/293/06 $2.00

were mixed in proportions that resulted in a final label percentage of ~10%, which was maintained constant for all experiments.

Three G-actin buffers were utilized in these experiments. They are designated as follows: G1 (2 mM Tris, 0.2 mM $CaCl_2$, 0.2 mM ATP, 0.5 mM DTT, 0.02% NaN_3), G2 (5 mM Tris, 0.1 mM $CaCl_2$, 0.5 mM ATP, 0.1 mM DTT, 0.02% NaN_3), G3 (5 mM Tris, 0.1 mM $MgCl_2$, 0.5 mM ATP, 0.1 mM DTT, 0.02% NaN_3). All buffers were prepared to have pH = 8.0 at 20°C. Distilled, deionized water was used throughout. The pH of each buffer was adjusted to the selected value by addition of HCl. All solution pH values were measured using a digital pH meter (model 601; Orion Scientific Instruments Corp., Pleasantville, NY) with a calibrated glass combination electrode. For the preparation of Mg-actin buffer, G3 was used throughout the actin preparation and column purification.

Pyrene-labeled actin increases in fluorescence yield upon transformation from globular to filamentous state, so the measurement of fluorescence intensity from an actin solution in assembly medium can be used to follow the progress of filament formation (Kouyama and Mihashi, 1981). For these experiments a small aliquot of the assembly salt was added to 2 ml of action solution in a fluorescence cuvette, the solution was mixed rapidly, and the cuvette was placed in a fluorescence spectrophotometer (model 650-10S; Perkin-Elmer Corp., Norwalk, CT). Fluorescence intensity was monitored at 388 nm (4-nm slit width) using 368-nm (2-nm slit width) illumination. Illumination was intermittent (typical duty cycle 3%) to minimize bleaching of the fluorophore. For quantitative comparisons of assembly kinetics, we determined the kinetic halftimes, defined as the time for the pyrene fluorescence signal to reach one-half of its eventual maximum value. As expected, halftimes were found to be a function of actin concentration, with a quasi–first-order dependence. For presentation of data from a wide variety of conditions (Table 1), half-times were corrected to a single concentration using the first-order approximation. This correction was never greater than 50%.

Critical concentrations of actin were also determined using the fluorescence yield increase of pyrene-labeled actin (Tobacman et al., 1983). Solutions of F-actin were sonicated at 50 W for 5 s and then diluted into the medium for which the critical concentration was to be determined. After 2 h the fluorescence intensity was determined as above for solutions over a range of actin concentrations. Plots of fluorescence intensity versus actin concentration were fitted by least-squares to two lines, the abscissa intercept of which is reported as the critical concentration.

Fluorescence photobleaching recovery (FPR) was also used to quantify the state of actin assembly as well as to determine the translational diffusion coefficients of actin filaments. The instrumentation and methodology have been described previously (Lanni et al., 1981; Lanni and Ware, 1982, 1984; Ware, 1984). Briefly, a trace quantity of fluorescein-labeled actin was incorporated with native actin. Polymerization was initiated by the addition of salt(s) to actin in buffer G1, and the sample was loaded into a microcuvette and placed onto the stage of a fluorescence microscope. For each measurement a striped pattern was photobleached into the specimen, and the contrast of the pattern was monitored as a function of time using a modulation detection scheme (Lanni and Ware, 1982). The decay in the amplitude of the modulation reflects the fading of the contrast of the pattern in the specimen as bleached and unbleached species randomize their positions by diffusion. From the FPR data we determined the relative proportion of rapidly and slowly diffusing actin (G-actin and F-actin, respectively), and the diffusion coefficients of the actin filaments. Successive measurements, always taken from different spatial regions in the specimen, may be recorded about once per minute, permitting kinetic resolution of the parameters determined. In the experiments presented here, data taken using a **K** vector ($2\pi/L$ where L is the period of the pattern in the specimen plane) of 841 cm^{-1} were fit by least squares to a single exponential (with fixed time constant appropriate for G-actin) plus a straight line to determine the proportion of immobile actin (from the relative amplitude of the straight line). Data taken using a **K** vector of 2,127 cm^{-1}, 4,254 cm^{-1}, or 6,381 cm^{-1} were fit to a single exponential plus a constant, with the time constant of the exponential interpreted to be $D\mathbf{K}^2$, where D is the average filament diffusion coefficient.

TABLE 1 Kinetic half-times (min) of actin assembly

Cation	pH 6.6	pH 7.4	pH 8.0
0.5 mM Mg^{+2}	4.1	56.0	310.0
0.75 mM Mg^{+2}	1.3	16.0	60.0
1 mM Mg^{+2}	2.7	6.9	19.0
1.25 mM Mg^{+2}	1.0	5.8	11.0
1.5 mM Mg^{+2}	1.3	4.5	8.8
2 mM Mg^{+2}	1.0	3.8	4.9
2 mM Ca^{+2}	3.2	13.0	23.0
3 mM Ca^{+2}	3.3	13.2	16.0
4 mM Ca^{+2}	2.8	5.7	20.7
5 mM Ca^{+2}	1.2	3.2	15.3
100 mM K^+	10.4	23.0	36.0
100 mM K^+ (0.1 mM Mg^{+2})	0.13	1.9	3.5

RESULTS

Kinetics of actin assembly were followed both by FPR and by pyrene–actin fluorescence enhancement. Sample data for both methods are shown in Fig. 1. For equivalent solution conditions the pyrene technique generally showed more rapid kinetics than the FPR method. The criteria for assembly are quite different: the pyrene technique reports an actin protomer conformational change that is thought to accompany assembly (Kouyama and Mihashi, 1981), whereas the FPR criterion is the hydrodynamic distinction between monomers and filaments (Lanni et al., 1981; Lanni and Ware, 1984). An analysis of the pyrene method in comparison to sedimentation assays has shown that the fluorescence signal is not exactly proportional to the incorporation of the monomers into filaments, but there was no indication of a substantial time lag (Grazi, 1985). We suspect that a significant component of the difference in time scale of the two signals may be a reduced rate of incorporation of fluorescein-labeled actin into the filament (Simon et al., 1988). The differences were greater at pH 8.0 than at pH 6.6, which we interpret to be a result of the titration of fluorescein to the anionic form. Nevertheless, both techniques demonstrate clearly and to approximately the same degree that actin assembly is substantially accelerated at lower pH. Data at the shortest times, available primarily from the pyrene assay, indicate that the more rapid kinetics at lower pH are attributable both to a reduced lag time and to a sharper slope in the elongation phase of assembly.

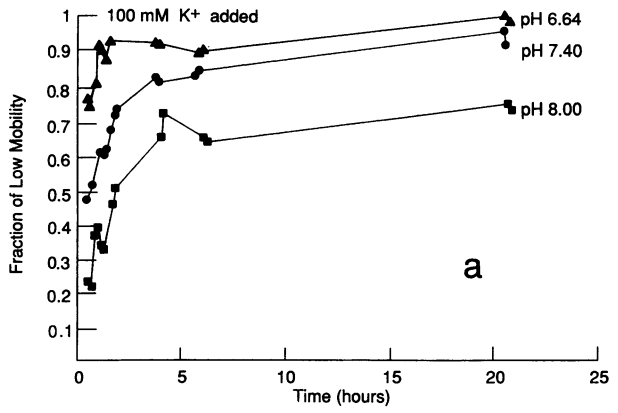

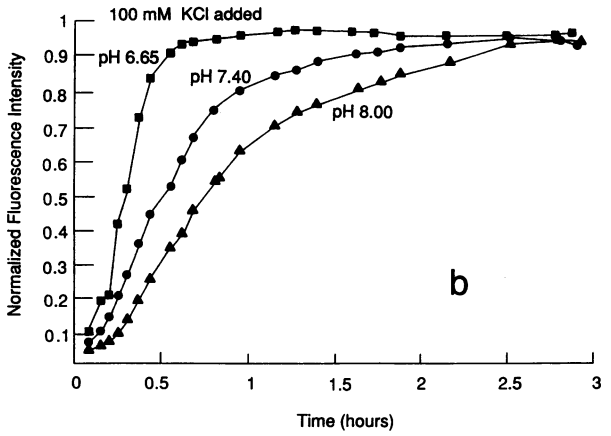

FIGURE 1 Sample data for actin assembly kinetics monitored by (*a*) FPR at the pH values of media shown. Actin concentration was 20.6 μM with 10.5% fluorescein labeled. 100 mM KCl was used to assemble the actin in buffer G1 and by (*b*) pyrene actin fluorescence enhancement at the pH values of media shown. Actin concentration was 7.62 μM with 10.8% pyrene labeled. 100 mM KCl was used to assemble the actin in buffer G2.

The kinetics of actin assembly are dramatically sensitive to the identity and concentration of the cations used to induce assembly. We have consequently examined the effects of pH on assembly kinetics for a variety of commonly employed ionic conditions. For most of these measurements the pyrene assay was deemed superior because of its better kinetic resolution, particularly for the early stages of assembly. In order to make convenient quantitative comparisons of assembly kinetics, we report the kinetic halftimes, i.e., the time for the pyrene fluorescence signal to reach one-half of its eventual maximum value. These kinetic halftimes for all of the conditions studied are shown in Table 1. All measurements were

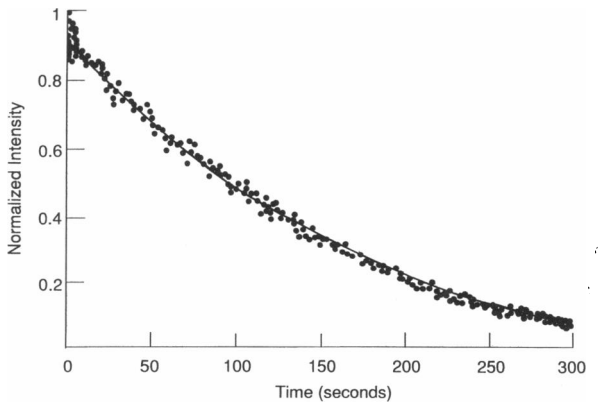

FIGURE 2 FPR trace for calculating the diffusion coefficient of filamentous actin. The trace was taken 7 h after addition of 100 mM KCl. The AC modulation envelope intensity in normalized units, which represents the contrast of the photobleached pattern, is plotted versus sampling time in seconds. The FPR data were fitted to a single exponential by least-squares method, and the fitted curve is shown.

performed at 20°C, and the halftimes shown correspond to a total actin concentration of 14 μM. The initial buffer (before addition of assembly salts) was buffer G2, except for the final entry, for which buffer G3 was used for the actin preparation and column filtration in order to prepare actin on which the tightly bound cation was Mg^{+2} instead of Ca^{+2}. The absolute magnitudes of the kinetic half times in Table 1 were reproducible to within about ±20% for the same sample of actin. Measurements using different preparations of actin differed by as much as a factor of 2 or more, but the relative trends with pH scaled about the same for all samples.

Filament diffusion coefficients were determined using FPR. A high **K** vector was selected so that the modulation decay from the relatively slowly diffusing filaments could be measured on a convenient time scale. A sample FPR trace is shown in Fig. 2. Data such as this were fitted by least-squares criterion to a single exponential with time constant given by $D\mathbf{K}^2$. Filament diffusion coefficients determined in this way for several ionic conditions and pH values are presented in Table 2. No systemic variation in filament diffusion coefficients with pH was observed.

TABLE 2 Diffusion coefficients of actin filaments (10^{-10} cm^{2}s^{-1})

Cation	pH 6.6	pH 7.0	pH 7.4	pH 7.7	pH 8.0
100 mM K^+	2.8	3.0	3.4	3.0	4.3
1 mM Mg^{+2}	7.7	4.4	6.4	3.3	4.8
100 mM K^+ 1 mM Mg^{+2}	4.4		3.6		3.1

A third parameter that may be used to quantify actin assembly is the critical concentration, i.e., the concentration of G-actin that remains unassembled in quasi-equilibrium with actin filaments. We have determined critical concentrations of actin under several different ionic conditions for pH 6.6, 7.4, and 8.0 using the pyrene fluorescence enhancement method described in the previous section. A typical plot of fluorescence versus concentration is shown in Fig. 3. In the example shown the slope of the line for filamentous actin is more than 12-fold greater than the slope for G-actin, making a determination of the intercept quite straightforward and precise. However, we have found that the ratio of these slopes is dependent both on the ionic conditions and on pH; for some conditions, particularly lower values of Mg^{+2}, the slope differences were not great enough to permit a reliable determination. In general we rejected data for which the ratio of slopes was less than 2. The critical concentrations that we were able to determine using this method are tabulated in Table 3. Again there is a clear and consistent trend, with lower critical concentrations at lower values of pH.

DISCUSSION

Over the range of conditions studied, increased acidity accelerates the kinetics of actin assembly and reduces the critical concentration. Both of these effects are present for all combinations of cations used in these experiments, but quantitative comparison reveals some dependence on the cations employed in the assembly medium. From pH 6.6 to 8.0 kinetic halftimes (Table 1) increased by as much as a factor of 75 (0.5 mM Mg^{+2}) to as little as a factor of 3 (100 mM K^+). When Mg^{+2} was used as the assembly ion, the relative increase of kinetic halftimes was reduced as the Mg^{+2} concentration was increased. This effect was not observed for assembly with Ca^{+2}, for which the kinetic halftime increased somewhat more with pH at the higher ion concentrations. When assembly was induced by 100 mM K^+, assembly kinetics were an order of magnitude more rapid and the kinetic halftime dependence was an order of magnitude greater when Mg^{+2} was the tightly bound cation than when Ca^{+2} was the tightly bound cation. The important distinction between Ca–actin and Mg–actin is well known, and the kinetic effects at a single pH (7.8) have been characterized in a recent report (Selden et al., 1986).

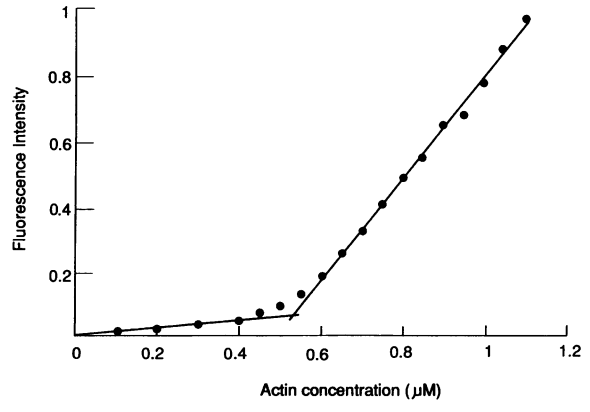

FIGURE 3 Sample data for determination of actin critical concentration. Fluorescence intensity from the pyrene label is plotted as a function of actin concentration. The data were fitted by least-squares criteria to two lines as shown. The abscissa intercept is the critical concentration. Solution conditions for these data were pH 7.40, buffer G3 + 1 mM $MgCl_2$.

TABLE 3 Actin critical concentrations (μM)

Cation	pH 6.6	pH 7.4	pH 8.0
1 mM Mg^{+2}	0.15	0.54	0.72
1.25 mM Mg^{+2}	0.11	0.36	0.49
4 mM Ca^{+2}	0.19	0.32	0.32
5 mM Mg^{+2}	0.17	0.19	0.26
100 mM K^+ 1 mM Mg^{+2}	0.081	0.10	0.22
100 mM K^+ 2 mM Mg^{+2}	0.070	0.10	0.11
100 mM K^+	0.36	0.44	0.62
100 mM K^+ (0.1 mM Mg^{+2})	0.17	0.20	0.24

From pH 6.6 to 8.0 the critical concentration of actin increased by as much as a factor of 5 and as little as a factor of 1.5. Again the greatest effect was seen when Mg^{+2} was used as the assembly ion, and the effect was greater for 1.0 mM Mg^{+2} than for 1.25 mM Mg^{+2}. For the conditions most closely resembling cytoplasmic conditions, the increase in critical concentration was a factor of 2.7 for (100 mM KCl, 1 mM $MgCl_2$) and a factor of 1.6 for (100 mM KCl, 0.2 mM $MgCl_2$). Changes in critical concentration of this magnitude could affect actin assembly and disassembly to a significant degree. Moreover, the presence of profilin or other G-actin–binding proteins in cytoplasm may greatly amplify the effects of small changes in the actin critical concentration on the concentration of F-actin (Tobacman and Korn, 1982).

Several of the critical concentration values in Table 3 may be compared with literature values. At pH 8.0, three sets of ionic conditions match conditions employed by Tobacman and Korn (1983) when introducing the method we have employed. Their values (with ours in parentheses) were 0.58 (0.72) for 1 mM $MgCl_2$, 0.76 (0.62) for 100 mM KCl + 0.1 mM $CaCl_2$, and 0.21 (0.22) for 100 mM KCl + 1 mM $MgCl_2$. The agreement appears to be quite close. Our values also agree well with

a previous report from this group (Pan and Ware, 1988), except for the values for 4 mM Ca^{+2} and 5 mM Ca^{+2}, which are about a factor of two lower in the present study. Selden et al. (1986) have measured critical concentrations for Mg–actin and Ca–actin at pH 7.8 using a polymerization plateau method and an initial rate method, both based on pyrene-labeled actin, but employing a different methodology. To the degree that direct comparisons can be made, their values appear to be lower than ours by a factor of 2–3. It is important to bear in mind that the critical concentration of actin has several definitions, both theoretically and experimentally. It has been shown to depend on the number concentration of actin filaments (Pantaloni et al., 1984), and it is the experience in our lab and elsewhere that it may depend on the preparation method and the age of the sample. From repeated measurements on all samples we find that the values in Table 3 are reproducible over all variables to within ±20%. Thus the relative trends with pH, which we are emphasizing in this report, are much larger than the experimental uncertainties.

The actin filament diffusion coefficients measured in an FPR experiment may be subject to several experimental artifacts, including photochemical reactions from the bleaching process. A detailed analysis of these effects has been published recently (Simon et al., 1988). However, we are confident that D_{LM} is a reliable, at least semiquantitative, index of relative filament length. In data not shown, we have verified that the D_{LM} decrease monotonically over three orders of magnitude as assembly proceeds and that their steady-state value is reproducible to within a factor of 2 or 3. We have also verified that mechanical shearing and various chemical and biochemical filament shortening agents have the appropriate effects on D_{LM} with a nearly linear dose dependence over about three orders of magnitude. The diffusion coefficients in Table 2 are within the range of reproducibility and thus do not show any measurable effect of pH or ion content on filament length. Some readers may find it surprising that conditions that favor more rapid assembly do not result in shorter filaments, but we have repeatedly found that kinetic effects and filament shortening effects are separable (Mozo-Villarias and Ware, 1984; Walling et al., 1988). Steady-state filament lengths are determined by a combination of factors that include the nucleation rate, cleavage rate, and annealing rate as well as rates of monomer association and dissociation. The lack of pH dependence of filament lengths has no unambiguous interpretation without further investigation.

The molecular interpretation of the pH dependence of actin assembly is presumed to be related to the titration of an anionic group(s) over this pH range. The fact that the pH dependence of critical concentrations and kinetic halftimes are affected for all combinations of assembling cations makes it seem likely that the sites involved are low-affinity sites with little specificity. Comparison of the quantitative data may support a special role for Mg^{+2} in interacting with these sites. It is known that Mg^{+2} induces a conformational change in G-actin (Frieden, 1982), and our observation that the pyrene fluorescence enhancement is sensitive to the level of Mg^{+2} present provides further evidence for that effect. Ultimate understanding of the conformational pH dependence will probably require an atomic resolution structure of G-actin and further spectroscopic characterizations of the individual titratable groups on the actin surface.

The immediate implications of our results are most important for the comparison of actin assembly measurements and the relation of measured parameters to cytoplasmic mechanisms. The pH is routinely controlled in actin experiments, but is rarely varied, and no standard value has been imposed. Comparisons of measured parameters generally do not include any corrections for pH dependences, and the application of measured parameters to cytoplasmic regulatory mechanisms generally do not consider the pH dependence or the variability of cytoplasmic pH. Our data show that the pH dependence of the assembly kinetics and critical concentrations of actin in a variety of media is sufficiently great that it should not be neglected. These considerations will become even more complex when combined with the pH dependence of cytoplasmic actin regulatory proteins.

Note added in proof: Following the submission of this manuscript, a report has appeared from another group on this same topic (Zimmerle, C. T., and C. Frieden. 1988. Effect of pH on the mechanism of actin polymerization. *Biochemistry.* 27:7766–7772). To the degree that direct comparisons can be made, we see no discrepancies between these two studies.

We are grateful to Professor D. Lansing Taylor for his suggestions and comments. This work was supported by Grant No. DMB-8607843 from the National Science Foundation.

Received for publication 18 July 1988 and in final form 6 October 1988.

REFERENCES

Barany, M., F. Finkelman, and T. Theratril-Antony. 1962. Studies on the bound calcium of actin. *Arch. Biochem. Biophys.* 98:28–45.

Bright, G. R., G. W. Fisher, J. Rogowska, and D. L. Taylor. 1987. Fluorescence ratio imaging microscopy: temporal and spatial measurements of cytoplasmic pH. *J. Cell Biol.* 104:1019–1033.

Busa, W. B. 1986. Mechanisms and consequences of pH-mediated cell regulation. *Annu. Rev. Physiol.* 48:389–402.

Carlier, M. F., D. Pantaloni, and E. D. Korn. 1986. The effects of Mg^{2+} at the high-affinity and low-affinity sites on the polymerization of

actin and associated ATP hydrolysis. *J. Biol. Chem.* 261:10785–10792.

Chaillet, J. R., K. Amsler, and W. F. Boron. 1986. Optical measurements of intracellular pH in single LLC-PKl cells: demonstration of Cl-HCO_3 exchange. *Proc. Natl. Acad. Sci. USA.* 83:522–526.

Drenckhahn, D., and T. D. Pollard. 1986. Elongation of actin filaments is a diffusion-limited reaction at the barbed end and is accelerated by inert macromolecules. *J. Biol. Chem.* 261:12754–12758.

Frelin, C., P. Vigne, A. Ladoux, and M. Lazdunski. 1988. The regulation of intracellular pH in cells from vertebrates. *Eur. J. Biochem.* 174:3–14.

Frieden, C. 1982. The Mg^{+2}-induced conformational change in rabbit skeletal-muscle G-actin. *J. Biol. Chem.* 257:2882–2886.

Grazi, E. 1985. Polymerization of N-(1-pyrenyl)iodoacetamide-labelled actin: the fluorescence signal is not directly proportional to the incorporation of monomer into the polymer. *Biochem. Biophys. Res. Commun.* 128:1058–1063.

Hartree, E. F. 1972. Determination of protein: a modification of the Lowry method that gives a linear photometric response. *Anal. Biochem.* 48:422–427.

Janmey, P. A., J. Peetermans, K. S. Zaner, T. P. Stossel, and T. Tanaka. 1986. Structure and mobility of actin filaments as measured by quasielastic light scattering, viscometry, and electron microscopy. *J. Biol. Chem.* 261:8357-8362.

Keiser, T., A. Schiller, and A. Wegner. 1986. Nonlinear increase of elongation rate of actin filaments with actin monomer concentration. *Biochemistry.* 25:4899–4906.

Korn, E. D. 1982. Actin polymerization and its regulation by proteins from nonmuscle cells. *Physiol. Rev.* 62:672–737.

Kouyama, T., and K. Mihashi. 1981. Fluorimetry study of N-(1-pyrenyl) iodoacetamide-labeled F-actin. Local structure change of actin protomer both on polymerization and on binding of heavy meromyosin. *Eur. J. Biochem.* 114:33–38.

Lanni, F., and B. R. Ware. 1982. Modulation detection of fluorescence photobleaching recovery. *Rev. Sci. Instrum.* 53:905–908.

Lanni, F., and B. R. Ware. 1984. Detection and characterization of actin monomers, oligomers, and filaments in solution by measurement of fluorescence photobleaching recovery. *Biophys. J.* 46:97–110.

Lanni, F., D. L. Taylor, and B. R. Ware. 1981. Fluorescence photobleaching recovery in solution of labeled actin. *Biophys. J.* 34:341–364.

Martonosi, A., C. M. Molino, and J. Gergeley. 1964. The binding of divalent cations to actin. *J. Biol. Chem.* 239:1057–1064.

Moolenaar, W. H. 1986. The regulation of cytoplasmic pH in human fibroblasts. *Annu. Rev. Physiol.* 48:363–376.

Mozo-Villarias, A., and B. R. Ware. 1984. Distinctions between mechanisms of cytochalasin D activity for Mg^{+2} and K^+-induced actin assembly. *J. Cell Biol.* 259:5549–5554.

Musgrove, E., C. Rugg, and D. Hedley. 1986. Flow cytometric measurement of cytoplasmic pH: a critical evaluation of available fluorochromes. *Cytometry.* 7:347–355.

Nuccitelli, R., and D. W. Deamer. 1982. Intracellular pH: Its Measurement, Regulation, and Utilization in Cellular Function. Alan R. Liss, Inc., New York.

Oosawa, F. 1983. Muscle and Non-Muscle Motility. A. Stracher, ed. Academic Press, Inc., New York. 151–216.

Pantaloni, D., M.-F. Carlier, M. Coué, A. A. Lal, S. L. Brenner, and E. D. Korn. 1984. The critical concentration of actin in the presence of ATP increases with the number concentration of filaments and approaches the critical concentration of actin · ADP. *J. Biol. Chem.* 259:6274–6283.

Pollard, T. D. 1981. Cytoplasmic contractile proteins. *J. Cell Biol.* 91:156s–165s.

Pan, X. X., and B. R. Ware. 1988. Actin assembly by lithium ions. *Biophys. J.* 53:11–16.

Pardee, J. D., and J. A. Spudich. 1982. Purification of muscle actin. *Methods Enzymol.* 85:164–181.

Selden, L. A., L. C. Gershman, and J. E. Estes. 1986. A kinetic comparison between Mg-actin and Ca-actin. *J. Musc. Res. Cell Motil.* 7:215–224.

Simon, J. R., A. Gough, E. Urbanik, F. Wang, B. R. Ware, and D. L. Taylor. 1988. Analysis of rhodamine and fluorescein-labeled F-actin diffusion in vitro by fluorescence photobleaching recovery. *Biophys. J.* 54:801–815.

Strzelecka-Golaszewska, H., E. Prochniewicz, and W. Drabikowski. 1978. Interaction of actin with divalent cations. The effect of various cations on the physical state of actin. *Eur. J. Biochem.* 88:219–237.

Tobacman, L. S., and E. D. Korn. 1982. The regulation of actin polymerization and the inhibition of monomeric actin ATPase activity by *Acanthamoeba* profilin. *J. Biol. Chem.* 257:4166–4170.

Tobacman, L. S., and E. D. Korn. 1983. The kinetics of actin nucleation and polymerization. *J. Biol. Chem.* 258:3207–3214.

Tobacman, L. S., S. L. Brenner, and E. D. Korn. 1983. Effect of *Acanthamoeba* profilin on the pre-steady state kinetics of actin polymerization and on the concentration of F-actin at steady state. *J. Biol. Chem.* 258:8806–8812.

Walling, E. A., G. A. Krafft, and B. R. Ware. 1988. Actin assembly activity of cytochalasins and cytochalasin analogs using fluorescence photobleaching recovery. *Arch. Biochem. Biophys.* 264:321–332.

Ware, B. R. 1984. Fluorescence photobleaching recovery. *Am. Lab. (Fairfield, Conn.)* 16:16–28.

Zaner, K. S., and J. H. Hartwig. 1988. The effect of filament shortening on the mechanical properties of gel-filtered actin. *J. Biol. Chem.* 263:4532–4536.